Journal of Applied Research and Technology

www.jart.icat.unam.mx

Journal of Applied Research and Technology 22 (2024) 1-8

Original

Active power compensator for a DC voltage bus of a renewable source

O. Morfín[a] • M. Gomez[a]* • J. Rodríguez[b] • M. Murillo[a] • N. Padilla[a]

[a]*Universidad Autónoma de Ciudad Juárez, Chihuahua, México*
[b]*The University of Texas at El Paso, USA*

Received 01 13 2023; accepted 06 13 2023
Available 02 29 2024

Abstract: Renewable energy sources generate intermittent electrical power due to weather conditions, such as variations in wind speed and solar radiation. The nature of renewable energy sources requires new techniques to maintain the quality of electrical service and efficient use of energy. One of these techniques uses a battery bank when a renewable energy source does not generate the power level contracted by the utility grid. This article proposes a power compensator consisting of a bidirectional DC converter located between the battery bank and the DC bus of a renewable source. This compensator has two operation modes: one to store the excessive power in a battery bank; the other to deliver power when power intermittency occurs. The validation of the proposed power compensator is made using a prototype where the DC voltage bus of a renewable energy source is emulated through a DC generator-motor set, which allows bidirectional power flow.

Keywords: active power compensator, bidirectional DC buck-boost converter, DC bus voltage emulator

*Corresponding author.
E-mail address: mgomez@uacj.mx (M. Gomez).
Peer Review under the responsibility of Universidad Nacional Autónoma de México.

1. Introduction

It is estimated that in the coming years the demand for energy will grow at a rate of 1.8% per year, until 2030, which represents a growth of 55% of the present global energy needs (Carta et al., 2009). Thus, to satisfy the growing power demand, societies must burn fossil fuels in large thermal power stations, increasing the pollution of the environment. To counterbalance pollution, engineers are searching for alternatives in power generation such as photovoltaic and wind power systems. These types of sources known as renewable energy sources have the feature of having intermittent power generation due to weather variability. One common approach to solve the intermittent problem is to use power compensator systems. A typical configuration of a power compensator uses a bidirectional DC-DC converter in conjunction with a battery bank for delivering power to a DC bus of a renewable power source when it does not meet the contracted energy demand. The Buck-Boost DC-DC converter controlled by PWM (pulse width modulation) signals has been used in DC-DC power converter applications (Guerra et al., 2021; Ham et al., 2019; Lopez-Garcia et al., 2018; Viswanatha & Venkata, 2018). The controllers of DC-DC Buck-Boost converters may be as simple as using comparators (Viswanatha & Venkata, 2018) or as complex as incorporating intelligent systems (Lopez-Garcia et al., 2018), and most of them regulate output voltage instead of power. In addition, the controllers have been used for tracking the maximum power point in photovoltaic systems. The maximum power point tracking algorithm could established the PWM duty cycle of a Buck-Boost converter using an intelligent technique applied in a photovoltaic system, as has been developed in (Guerra et al., 2021); the photovoltaic system was modeled, and several weather conditions were evaluated to analyze the output power. The load value and the maximum power point were considered to calculate the output voltage of the photovoltaic system. A DC-DC Buck-Boost controller for the charging and discharging of a battery using the microcontroller 8051 has been developed in (Viswanatha & Venkata, 2018), by sensing the voltage across the load to regulate the output voltage. A DC-DC Buck-Boost converter to deliver current to a DC bus, whose controller is based on recurrent high-order neural networks, has been proposed in (Lopez-Garcia et al., 2018); a single control law has been formulated for tracking the power reference by setting a current reference for battery charge and another one for discharge; the controller was implemented with the Texas Instruments F28069M launchpad which includes an enhanced pulse width modulator; large errors were shown due to an overshoot in the response.

This paper is structured in the following way. Section 2 describes the power compensator connected to a DC bus. In Section 3, the model of a bidirectional DC-DC converter is described. Section 4 shows the design of the power controller. In Section 5, a DC bus voltage emulator is proposed. Section 6 analyzes the performance of the power compensator through a set of experiments. Finally, conclusions are presented.

2. Power compensator system

In the case when a renewable energy source has a shortage in the generated power due to weather conditions, a power compensator can deliver the missing power. The topology of a renewable energy source connected to the utility grid involving an active power compensator is depicted in Figure 1 (Viswanatha & Venkata, 2018). The photovoltaic system is connected to the utility grid through a three-phase inverter and an LCL filter. Whereas the bidirectional power compensator is connected to the DC bus of the renewable energy source and is constituted by a battery bank and a bidirectional DC converter in a Buck-Boost configuration (Viswanatha & Venkata, 2018).

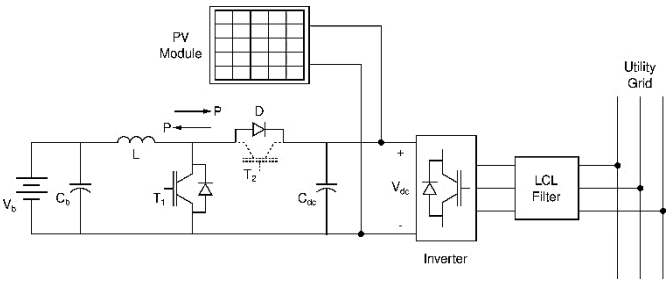

Figure 1. Photovoltaic system with power compensator.

When there is a reduction in the generated power by the renewable energy source, then the bidirectional DC converter operates in boost mode, where T_1 is activated to deliver power from the batteries to the DC bus. On the other hand, when there is a surplus in the generated power, the power is stored in the battery bank via the activation of the transistor T_2 in buck mode.

3. Bidirectional DC-DC converter

The bidirectional DC-DC converter works in boost mode when regulated power is delivered to the DC bus from the battery bank. On the other hand, this converter works in buck mode when the energy is stored in the battery bank at a regulated power level, which is supplied from the utility grid through the DC bus. Having the bidirectional power flow, the DC bus voltage tends to go up or down depending on the process of receiving or delivering power, however, the grid-side inverter controller of a renewable energy source regulates the DC bus voltage to a constant level (Morfin et al., 2016).

3.1. Bidirectional DC converter in boost mode

The topology of the DC boost converter is shown in Figure 2. From the input node, the equation of currents is set as:

$$-i_b + C_b \frac{d}{dt} v_{C_b} + i_L = 0 \tag{1}$$

The Eq. 1 is defined independently of the operation mode of transistor T_1. Meanwhile, a second equation, now of voltages, which fulfills both operation modes of the transistor T_1 (on and off), is:

$$-v_b + L \frac{d}{dt} i_L + (1-u) v_{dc} = 0 \tag{2}$$

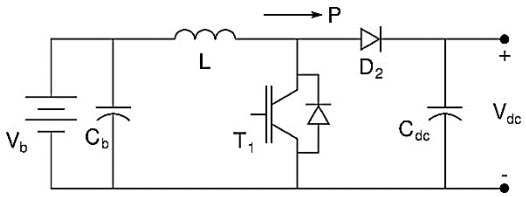

Figure 2. Topology of the DC boost converter.

Joining Eqs. 1 and 2, the average model of the power compensator in boost mode takes the following form (Sira-Ramirez & Silva-Ortigoza, 2006):

$$\begin{aligned} \frac{d}{dt} v_{C_b} &= -\frac{1}{C_b} i_L + \frac{1}{C_b} i_b \\ \frac{d}{dt} i_L &= -\frac{1}{L}(v_{dc} - v_b) + \frac{1}{L} v_{dc} u \end{aligned} \tag{3}$$

where $u = 1$ when the transistor T_1 is on and $u = 0$ for T_1 off, u commutates at high frequency and it is the duty cycle of the PWM signal, as the control input, i_L and i_b are the inductor and battery current, respectively; and v_b and v_{dc} are the battery and DC bus voltage, respectively.

3.2. Bidirectional DC converter in buck mode

The topology of the DC buck converter is shown in Figure 3. In this converter, the output node is the same as the input node in the DC boost mode, then, the current equation results in:

$$-i_L + C_b \frac{d}{dt} v_{C_b} + i_b = 0 \tag{4}$$

In addition, the voltage equation that fulfills both operation modes of the transistor T_2 (on and off), is:

$$-u v_{dc} + L \frac{d}{dt} i_L + v_b = 0 \tag{5}$$

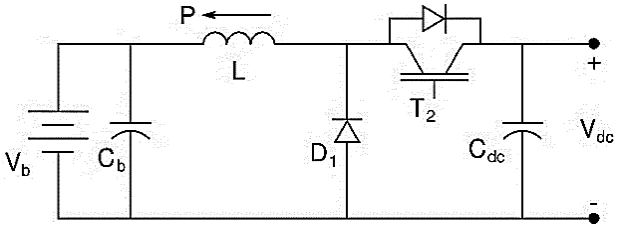

Figure 3. Topology of the DC buck converter.

Joining Eqs. 4 and 5, the average model of the power compensator in buck configuration results in (Sira-Ramirez & Silva-Ortigoza, 2006):

$$\begin{aligned} \frac{d}{dt} v_{C_b} &= \frac{1}{C_b} i_L - \frac{1}{C_b} i_b \\ \frac{d}{dt} i_L &= -\frac{1}{L} v_b + \frac{1}{L} v_{dc} u \end{aligned} \tag{6}$$

Buck model, described by Eq. 6, is very similar to the boost model, Eq. 3, nevertheless, the control input in the buck model needs less energy for canceling only the batteries voltage; meanwhile, the control input in the boost model needs more energy due to it cancels the difference between the DC bus voltage and the batteries voltage.

4. Design of power controller

The power controller design starts by defining a power error variable, then, the dynamics of the power error are defined, where the corresponding DC converter model is involved. When the power reference has a plus sign, the compensator delivers power toward the utility grid through the DC voltage bus, and the boost configuration of the bidirectional converter is used. When the power reference has a minus sign, the compensator stores the exceeding power from the utility grid, and the buck configuration is used.

4.1. Power controller in the boost configuration

The first step to designing the power controller consists of defining a power error variable as follows:

$$\varepsilon_p = p_{ref} - p_{in} = p_{ref} - v_b i_L \tag{7}$$

whose dynamics is:

$$\dot{\varepsilon}_p = \dot{p}_{ref} - \dot{p}_{in} \tag{8}$$

With the application of the power controller, the regulation problem is solved, where the set-point is constant, therefore substituting Eq. 7 into Eq. 8 the error dynamics takes the form:

$$\dot{\varepsilon}_p = -v_b \frac{d}{dt} i_L \tag{9}$$

involving the boost model (Eq. 3) in Eq. 9 yields:

$$\dot{\varepsilon}_p = \frac{1}{L} v_b (v_{dc} - v_b) - \frac{1}{L} v_b v_{dc} u \tag{10}$$

applying the proportional-integral controller:

$$u = K_p \varepsilon_p + K_i \int_0^t \varepsilon_p d\tau \tag{11}$$

in Eq. 10, the power error tends to zero asymptotically, as follows:

$$\dot{\varepsilon}_p = -K_1 \varepsilon_p \tag{12}$$

where K_1 defines the rate of convergence.

Involving the proportional integral control law of Eq. 11 into system of Eq. 10, we obtain the next:

$$\begin{aligned} \frac{d}{dt} i_L &= -\frac{1}{L}(v_{dc} - v_b) \\ &+ \frac{1}{L} v_{dc} \left[K_p (p_{ref} - v_b i_L) + K_i q \right] \\ \dot{q} &= p_{ref} - v_b i_L \end{aligned} \tag{13}$$

then applying Laplace transform transformation to Eq. 13, results in:

$$\begin{aligned} sI_L = \frac{1}{L} V_{dc} \Big[& K_p P_{ref} - K_p V_b I_L + K_i \frac{P_{ref}}{s} \\ & - K_i V_b \frac{I_L}{s} \Big] - \frac{1}{L}(V_{dc} - V_b) \end{aligned} \tag{14}$$

The system (Eq. 14) is pictured in Figure 4, and it has two inputs, which are p_{ref} and (V_{dc}-V_b), but applying the superposition principle, the following transfer function can be obtained:

$$\begin{aligned} G(s) &= \frac{I_L(s)}{P_{ref}(s)} \\ &= \frac{\frac{K_p v_{dc}}{L} s + \frac{K_i v_{dc}}{L}}{s^2 + \frac{K_p v_{dc} v_b}{L} s + \frac{K_i v_{dc} v_b}{L}} \end{aligned} \tag{15}$$

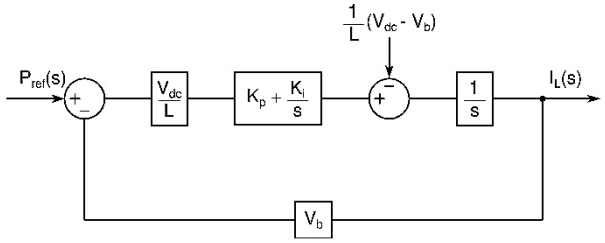

Figure 4. Boost power controller scheme.

Applying the Routh stability test (Franklin et al., 2002), the gains of the proportional-integral controller must satisfy:

$$\begin{aligned} K_p &> 0 \\ K_i &> 0 \end{aligned} \tag{16}$$

nevertheless, analyzing Eq. 10 in steady state, the control input is:

$$u_{ss} = 1 - \frac{v_b}{v_{dc}} \tag{17}$$

which defines the duty cycle of the PWM signal when the battery bank delivers power to the DC voltage bus.

4.2. Power controller in the buck configuration

The power error variable is:

$$\varepsilon_p = p_{ref} - p_{out} = p_{ref} - v_b i_L \tag{18}$$

and the dynamics of this power error variable is:

$$\dot{\varepsilon}_p = -v_b \frac{d}{dt} i_L \tag{19}$$

involving the buck model (Eq. 6) in Eq. 19 results in:

$$\dot{\varepsilon}_p = \frac{1}{L} v_b^2 - \frac{1}{L} v_b v_{dc} u \tag{20}$$

applying the proportional-integral controller:

$$u = K_p \varepsilon_p + K_i \int_0^t \varepsilon_p d\tau \tag{21}$$

in Eq. 20, the power error variable tends to zero in asymptotical form:

$$\dot{\varepsilon}_p = -K_2 \varepsilon_p \tag{22}$$

where K_2 is the pole that defines the speed of convergence.

The system (Eq. 20) has the form as Eq. 10; therefore, applying the Routh stability test (Franklin et al., 2002), the gains of the controller satisfy:

$$K_p > 0 \qquad K_i > 0 \tag{23}$$

and analyzing Eq. 20 in steady state, the control input is:

$$u_{ss} = \frac{v_b}{v_{dc}} \tag{24}$$

which defines the duty cycle of the PWM signal when the battery bank stores power delivered by the DC voltage bus.

5. DC bus voltage emulator

The emulation of the DC bus voltage of a renewable energy source can be done through a motor-generator set to establish a bidirectional flow of the electric power. In this project, an impulsion motor is coupled with a DC generator via a belt, where an analog proportional-integral controller regulates the generator voltage. To define the input-output DC generator model, the output response of the voltage generator is obtained from a step input voltage applied to the field winding, as is shown in Figure 5 (Franklin et al., 2002).

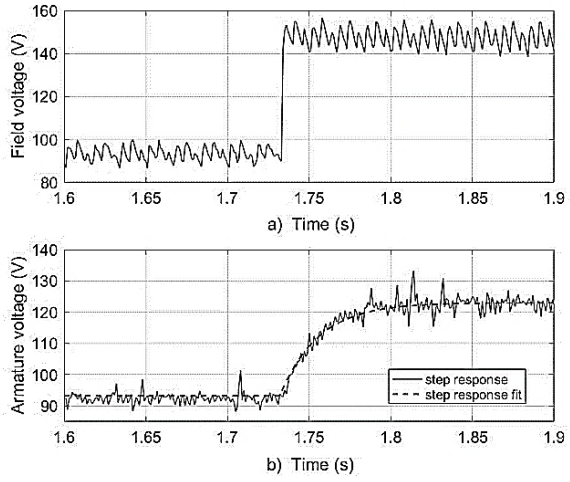

Figure 5. Step response of the DC generator.

The step response of the armature voltage can be modeled with the function:

$$y(t) = 93.2 + 29.81[1 - e^{-42.58(t-1.732)}]u(t-1.732) \tag{25}$$

The maximum slope of the step model (Eq. 25) is:

$$R = \left.\frac{dy}{dy}\right|_{t=1.732} = (-29.81)(-42.58) = 1269.3 \tag{26}$$

and the delay time of the step response model is approximately:

$$L \approx 0.01 \tag{27}$$

from Figure 5b, the approximate first-order transfer function that defines this response is:

$$H(s) = \frac{V_a(s)}{V_f(s)} = \frac{42.58 + 0.76s}{s + 42.58} \tag{28}$$

This model is obtained from output voltage data measured in the generator terminals (Figure 5b) under the step test of the input voltage applied to the field winding (Figure 5a). The closed-loop function transfer involving the proportional-integral DC voltage controller yields:

$$G(s) = \frac{V_a(s)}{V_{ref}(s)} = \frac{\left(K_p + \frac{K_i}{s}\right)\left(\frac{42.58 + 0.76s}{s + 42.58}\right)}{1 + \left(K_p + \frac{K_i}{s}\right)\left(\frac{42.58 + 0.76s}{s + 42.58}\right)} \tag{29}$$

whose characteristic equation takes the form:

$$s^2 + \frac{(0.76K_i + 42.58K_p)}{1 + 0.76K_p}s + \frac{42.58K_i}{1 + 0.76K_p} = 0 \tag{30}$$

applying the Routh stability test (Franklin et al., 2002), the gains of the proportional-integral controller must satisfy:

$$K_p > -0.017K_i \qquad K_i > 0 \tag{31}$$

Based on the Ziegler-Nichols method tuning (Ogata, 2010), the proportional-integral gains are defined as:

$$K_p = \frac{0.9}{RL} = \frac{0.9}{(1383.65)(0.01)} = 0.06$$

$$K_i = \frac{0.3}{L}K_p = \frac{0.3}{0.01}(0.06) = 1.8 \quad (32)$$

6. Experimental results

The experimental tests to validate the power compensator performance were made using the academic LabVolt equipment and the kit dSPACE 1103. The specific hardware used, the characteristics of the program, and the parameters of the DC bidirectional converter are presented in this section.

6.1. Control system of the power compensator

The performance of the bidirectional power compensator is validated experimentally in the laboratory using the academic LabVolt equipment, which is controlled by the kit dSPACE 1103, see Figure 6. The LabVolt equipment works with modules, in the left side column are located the voltage and current sensors, and in the middle column are the batteries bank and the drive for the boost configuration, meanwhile in the right-side column is the input of the DC bus voltage, the drive for the buck configuration, and in the upper part are the inductor and capacitor of the converter. On the left side of the display is located the input-output interface with the signaling LEDs of the kit dSPACE 1103, on the display is running the software Controldesk which is used to supervise the performance of the power compensator, showing the output variables, and tuning the gains of the power controller.

The base program is codified in Simulink/MATLAB using a sample time of 40 µs and a PWM frequency of 5 kHz, for conditioning of the signal control. The controller gains were tuned as follows: the proportional term, K_p = 0.0026, and the integral term, K_i = 0.0036, for both proposed controllers.

Finally, Figure 7 shows the voltage levels of the batteries bank and DC bus, and the parameters of the bidirectional DC buck-boost converter, which was connected using the LabVolt equipment.

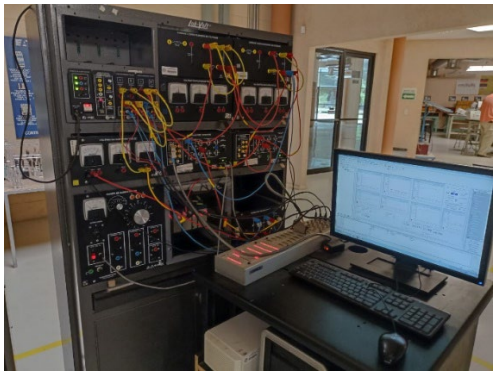

Figure 6. Power compensator prototype.

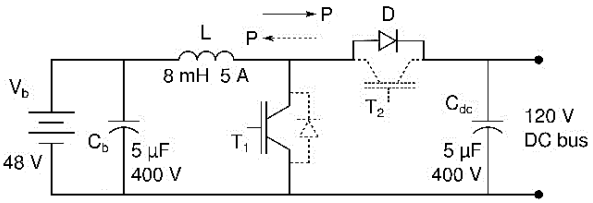

Figure 7. Parameters of the bidirectional DC converter.

6.2. Controller of the compensator in boost mode

The performance of the power compensator in boost mode is done in an effective way, as is shown in Figure 8. Two steps are presented, one of them from 40 W to 45 W, and another from 45 W to 50 W. The tracking of the power reference is effective with a settling time of 1.7 s, without an overshot. Consider that the capacity of the DC generator is 180 W, with which the DC bus voltage of the renewable energy source is emulated.

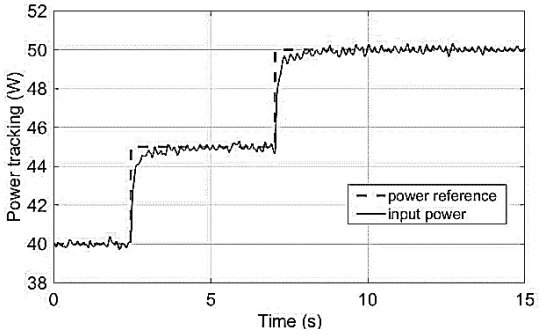

Figure 8. Boost power compensator performance.

The power controller behaves efficiently when a disturbance is presented, as is the case of changing the power reference, which is pictured in Figure 9. The duty cycle, as control input, varies slightly around 0.72.

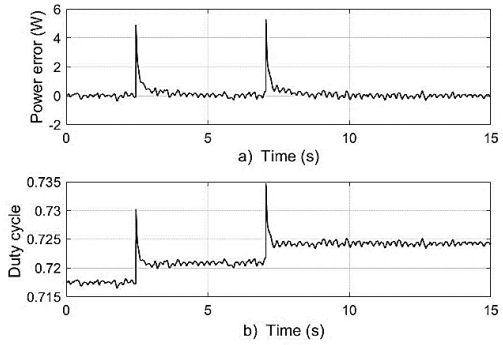

Figure 9. Boost power controller performance.

In Figure 10, the power changes and their corresponding current changes in the batteries are shown, as predicted by the transference function *G(s)* (Eq. 15).

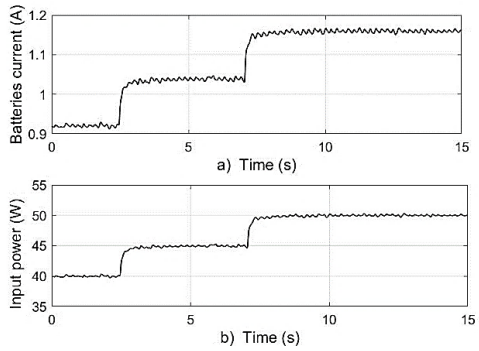

Figure 10. Batteries power and current in boost mode.

The DC bus voltage is emulated by a DC motor-generator set with a controlled output voltage of approximately 120 V, in the presence of disturbances, as is seen in Figure 11.

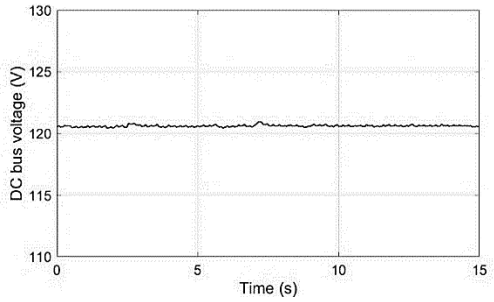

Figure 11. Controlled DC bus voltage in boost mode.

6.3. Controller of the compensator in mode buck

The performance of the power compensator in buck mode boost configuration is effective, as can be seen in Figure 12. The power tracking is like boost mode with the same two steps in the power reference, one of them from 40 W to 45 W, and another from 45 W to 50 W. The tracking of the power reference is effective with a settling time, less than boost mode, of 1.2 s, without an overshoot.

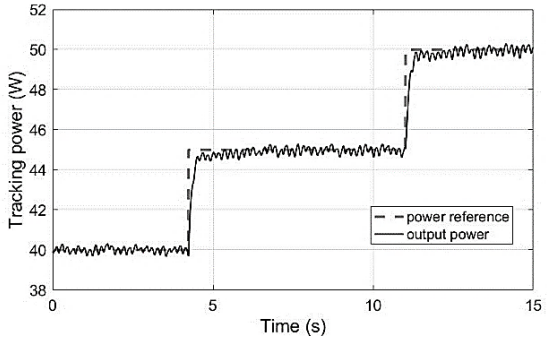

Figure 12. Buck power compensator performance.

The power controller cancels in an effective way the disturbances, as is the case of changing the power reference which is shown in Figure 13. The duty cycle, as control input, varies slightly around 0.47.

The power changes and, their corresponding, current changes in the batteries are shown in Figure 14.

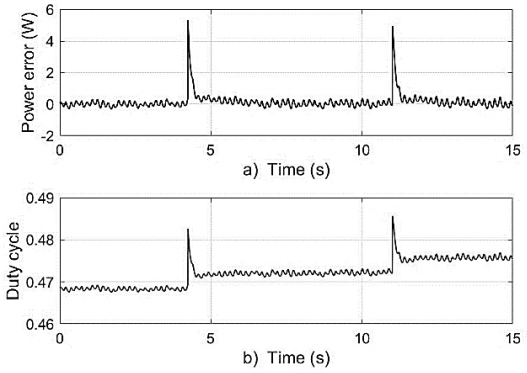

Figure 13. Buck power controller performance.

The DC bus voltage is maintained at 120 V in presence of disturbances, with which the output voltage control of the generator is corroborated, then the DC voltage bus is satisfactorily emulated, see Figure 15.

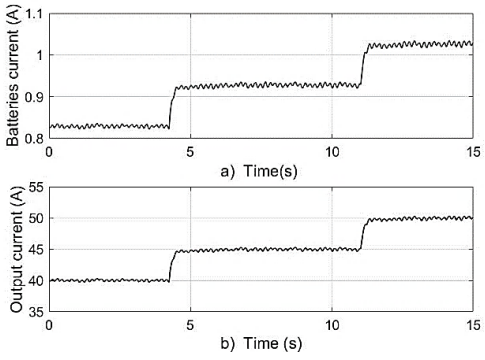

Figure 14. Batteries power and current in buck mode.

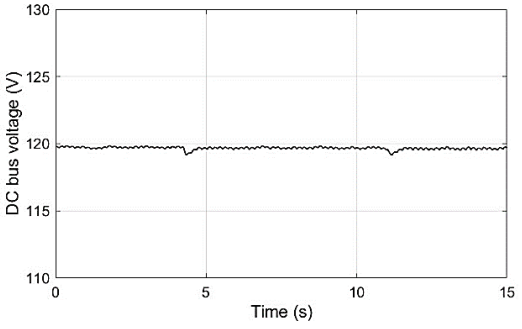

Figure 15. Controlled DC bus voltage in buck mode.

6.4. DC bus voltage emulator

The prototype of the DC bus voltage emulator is configured with the LabVolt equipment. This emulator is composed by a DC impulsion motor coupled to a DC generator through a belt, an H-bridge DC converter, and an analogic proportional-integral DC voltage controller, as shown in Figure 16. In the left side column are the voltage and current sensors and the DC power supply, in the middle column are the analogical PI controller, the H-bridge DC converter and the DC impulsion motor, and in the right-side column is the DC generator with the controlled output voltage.

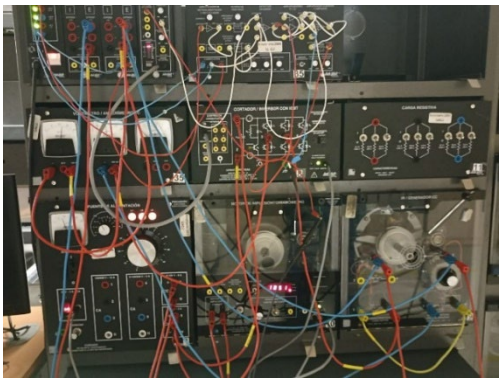

Figure 16. Prototype of the DC bus emulator.

7. Conclusions

This article proposes a prototype of a bidirectional power converter to compensate the generated electrical energy provided by a renewable energy source. The power controller has an effective performance when it regulates the power in both operation modes, in boost and buck configuration. The active power compensator is a solution when a renewable energy source does not generate the power level committed to the utility grid by supplying the needed energy.

Conflict of interest

The authors have no conflict of interest to declare.

Acknowledgements

We would like to express our sincere gratitude to the Electrical Engineering Laboratory at the Department of Electrical Engineering and Computer Science, Institute of Engineering and Technology of the Autonomous University of Ciudad Juárez, for their invaluable support in conducting the experimentation using the LabVolt academic equipment. Their assistance and resources contributed to the successful completion of this research.

Funding

The authors received no specific funding for this work.

References

Carta, J. A., Castro, M. A., Collado, E., & Calero, R. (2009). *Centrales de energías renovables: generación eléctrica con energías renovables.* Madrid: Pearson Educación, S. A.

Franklin, G. F., Powell, J. D., Emami-Naeini, A., & Powell, J. D. (2002). *Feedback control of dynamic systems* (Vol. 4). Upper Saddle River: Prentice hall.

Guerra, M. I., Ugulino de Araújo, F. M., Dhimish, M., & Vieira, R. G. (2021). Assessing maximum power point tracking intelligent techniques on a PV system with a buck–boost converter. *Energies*, *14*(22), 7453. https://doi.org/10.3390/en14227453

Ham, S. H., Choi, Y. G., Lee, H. S., Lee, S. W., Lee, S. C., & Kang, B. (2019). High-efficiency Bidirectional Buck–Boost Converter for Residential Energy Storage System. *Energies*, *12*(19), 3786. https://doi.org/10.3390/en12193786

Lopez-Garcia, T. B., Ruiz-Cruz, R., & Sanchez, E. N. (2018). Real-time battery bank charge-discharge using neural sliding mode control. In *2018 International Joint Conference on Neural Networks (IJCNN)* (pp. 1-8). IEEE. https://doi.org/10.1109/IJCNN.2018.8489533

Morfin, O. A., Ornelas-Tellez, F., Ruiz-Cruz, R., Castañeda, C. E., Murillo, M. A., & Sanchez, J. (2016). Decentralized control scheme for a photovoltaic system connected to the utility grid. In *2016 IEEE PES Transmission & Distribution Conference and Exposition-Latin America (PES T&D-LA)* (pp. 1-6). IEEE. https://doi.org/10.1109/TDC-LA.2016.7805690

Ogata, K. (2010). *Modern Control Engineering.* New Jersey: Prentice Hall.

Sira-Ramirez, H. J., & Silva-Ortigoza, R. (2006). *Control design techniques in power electronics devices.* Springer Science & Business Media.

Viswanatha, V. & Venkata, R. (2018). Microcontroller based bidirectional buck–boost converter for photo-voltaic power plant. *Journal of Electrical Systems and Information Technology*, *5*(3), 745-758. https://doi.org/10.1016/j.jesit.2017.04.002